Proceedings of the 9th International Conference on Aluminium Alloys (2004)
Edited by J.F. Nie, A.J. Morton and B.C. Muddle

Aluminium Powder Forging Process using a Rotating Platen

S.S. Youn[1], J.H. Park[2], C.W. Park[1], Y.H. Kim[1], X. Ma[3]

[1]ERC/NSDM, School of Mechanical Engineering, Pusan National University Jangjeon-Dong, Kumjeong-Ku, Pusan 609-735, Korea
[2]Research Institute of Mechanical Technology, Pusan National University Jangjeon-Dong, Kumjeong-Ku, Pusan 609-735, Korea
[3]School of Engineering and Technology, Deakin University, Geelong, VIC 3217, Australia

Keywords: Torsional Upset Forging, Sintered Structure, Upper Bound Analysis, Bulging Effect, Densification

Abstract

A torsional upset forging process is analysed on the basis of plasticity theory for powder metal forging. Torsional upset forging is a process to be performed by rotating a lower die with a punch travelling along the longitudinal direction of a work-piece. In this study, an upper bound analysis considering bulging effect, finite element method simulation (DEFORM^{3D}), and experimental research have been performed for the process. A simple kinematically admissible velocity field for a three dimensional deformation is presented for the torsional upset forging of a cylindrical billet. Distributions of stress, strain, and forging load in the process have been obtained, and compared with those in conventional upset forging. In the process, an increase in a friction factor and rotation speed results in a decrease in magnitude of upset force, dead metal zone, and non-homogeneous deformation. This process can reduce forming load, which leads to improvement of die life, and also reduce bulging effect. In addition, the initial sintered-structure and density distribution is improved by the process and surface defect due to high deformation is decreased.

1. Introduction

A powder forging method is a combined process of P/M (Powder Metallurgy) and precision forging, which takes advantage of them. Due to 10-20% of porosity in products by P/M, they have such lower ductility, fatigue strength, and impact strength that their dimension and application have a kind of limitation [1]. However, the limitation caused by lower mechanical properties can be overcome by adopting a powder forging process. In a powder forging process, a preform made by sintering goes through a forging process, so that an increase in density over the whole product and strengthened mechanical properties can be achieved. This also leads to a fine microstructure, a lightweight products and less energy and material. Because of these advantages, the process is being studied as an alternative for parts used in vehicle and aircraft.

In these days, various researches have been performed aiming at new methods that are capable of reducing forming load and induce more uniform deformation by positive application of friction at forging. Among them, torsional upset forging is a combined process of a vertical movement of a punch and a rotational movement of a die. Experiments and finite element (FE) simulations were carried out on solid materials for this process by Xue et al [2], Park et al [3] and Kemin et al [4].

Upper bound solutions were also obtained by Kim et al [5] and Ma et al [6] in which reductions in load and barrelling were reproduced. In this study, torsional upset forging is used with purpose to achieve uniform distribution of density during forging of powder metal. Upper bound analysis including the effect of hydrostatic pressure, laboratory tests, and FE simulation are carried out. Results of torsional upset forging are shown to be superior to those of conventional forging.

2. Theoretical Background

Among yield criteria of powder metal, Shima-Oyane's criterion is used in this study [7]:

$$\Phi^2 = \frac{1}{2}\left\{(\sigma_{11}-\sigma_{22})^2 + (\sigma_{22}-\sigma_{33})^2 + (\sigma_{33}-\sigma_{11})^2\right\} + \left(\frac{\sigma_m}{f}\right)^2 \tag{1}$$

Here, σ_{11}, σ_{22}, σ_{33} are principal stresses, σ_m is the hydrostatic stress, $f = 1/\left(2.5\sqrt{1-\rho}\right)$(ρ: relative density), and Φ is the plastic potential.

Relationship between the stress and strain tensor components σ_{ij} and ε_{ij} (i, j =1-3) is expressed as:

$$d\varepsilon_{ij} = d\lambda' \frac{\partial \Phi}{\partial \sigma_{ij}} = d\lambda\left[\sigma_{ij} - \left(1 - \frac{2}{9f^2}\right)\sigma_m\right] \tag{2}$$

Incremental volumetric strain is shown as:

$$d\varepsilon_v = d\varepsilon_{11} + d\varepsilon_{22} + d\varepsilon_{33} = -\frac{d\rho}{\rho} = \frac{dV}{V} = d\lambda \frac{2}{3f^2}\sigma_m \tag{3}$$

3. Upper Bound Analysis

Schematic drawings of analytical models for torsional upset forging are shown in Figure 1.

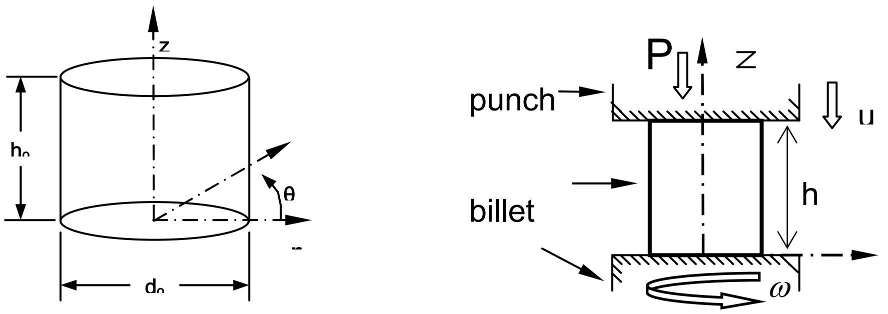

Figure 1: Schematic drawings of analytical models of torsional upset forging.

(a) geometry of the initial billet (b) schematic drawing of experimental equipment

Kinematically admissible velocity field is determined under the following assumptions: (a) the circumferential velocity component is not vanishing due to material twisting, and the radial velocity varies with the height of the billet; (b) the friction factor, m, is constant during deformation; (c) the volume of the billet varies with the densification; and the material yielding conforms with the Shima-Oyane's criterion in which the hydrostatic stress affects yielding, but the material is perfectly plastic and isotropic and (d) the plastic deformation is incremental, and the density is uniform in the deformed body. The determined velocity field in the cylindrical coordinate system (r, z, θ) of Fig. 1(a) is as follows.

$$v_r = AB\left(1-\beta z^2\right)\cdot r\,,\ v_\theta = ar\omega \cdot \frac{h-z}{h},\ v_z = -2Az\cdot\left(1-\beta z^2/3\right) \tag{4}$$

$$A = \frac{U}{2h\left(1-\beta h^2/3\right)} \tag{5}$$

Here, A is determined from the boundary condition and *B* is coefficient to indicate plastic flow of a specific material according to the relative density (1 for the conventional metals, 0~1 for sintered metal); *a* is slip factor which is the ratio of rotation speeds between a billet and a die; ω is the angular velocity of the die; *U* is the compression speed; and β is the bulging coefficient.

The rate of total energy dissipation for the torsional upset forging can be expressed as:

$$J^* = \dot{W}_i + \dot{W}_f - \dot{W}_m = PU \tag{6}$$

where the rate of internal energy dissipation $\dot{W}_i$ is calculated as:

$$\dot{W}_i = \int_V \overline{\sigma}\dot{\overline{\varepsilon}} dV \tag{7}$$

Here, $\overline{\sigma}$ is the effective stress, -$\dot{\overline{\varepsilon}}$ is the effective strain rate which can be determined from the kinematically admissible velocity field in Eq (4), and *V* is the volume of testpiece. The rate of frictional shear energy losses $\dot{W}_f$ is shown as:

$$\dot{W}_f = \int_{S_f} m\frac{\overline{\sigma}}{\sqrt{3}}\left|\Delta V_f\right| dS_f \tag{8}$$

Here, $\left|\Delta V_f\right|$ is the velocity discontinuity at the contact surface S_f between the billet and the die, which can occur on the upper and lower contact surfaces and can be calculated as:

$$\text{z=h: } \left|\Delta V_{punch}\right| = AB(1-\beta h^2)r \tag{9}$$

$$\text{z=0: } \left|\Delta V_{die}\right| = \sqrt{(ABr)^2 + ((1-a)rw)^2} \tag{10}$$

The rate of moment energy supplied by the rotation of the lower die $\dot{W}_m$ is determined as:

$$\dot{W}_m = M\cdot\omega = \frac{m}{\sqrt{3}}\int_{S_t} \frac{ar^2\omega^2}{\sqrt{(ABr)^2 + (ar\omega)^2}}\overline{\sigma} ds_t \tag{11}$$

Inserting Eqs. (7), (8) and (11) into Eqs. (6) gives an expression for the compression load *P.* This expression can be solved numerically and the corresponding solution obtained will be compared with that from the tests and FE simulation in Section 5.

4. Experiments

Alumix123 (Al-4.5 Cu-0.5 Mg-0.7Si) produced by ECKART Co., Germany, is selected as the test powder metal for the present experiments. This powder metal contains 1.5% micro wax as lubricant, and the other properties are shown in Table 1. The powder is then compacted using the die set as shown in Figure 2. The specimens are inserted into the sintering furnace, maintained at 400°C for 30 minutes to remove wax, and then directly heated up to 580°C for 25 minutes to be sintered. After sintering, the pieces are cooled down to 150°C, and then air cooled to 40°C. N_2 gas was used to fabricate the specimens as atmosphere one. The sintered products are shown in Figure 3.

Table 1 Typical physical characteristics of Alumix123

Apparent density [g/cm^3]	Tap density [g/cm^3]	Green Strength [N/mm^2]
1.0	1.3	>8.0

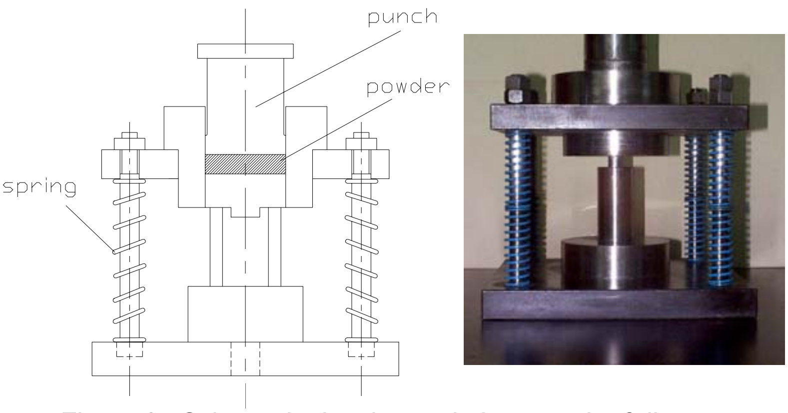

Figure 2: Schematic drawing and photograph of die set

The equation for flow stress is assumed as a function of strain rate and determined by hot compression tests of the sintered specimens using MTS, which is expressed as:

$$\bar{\sigma} = 36.5 \cdot \dot{\bar{\varepsilon}}^{0.155}\,[MPa] \tag{12}$$

In the torsional upset forging experiment, the punch velocity is 1 mm/s and the angular velocities of the lower die are varied with the other experimental conditions as shown in Table 2.

Figure 3: Photograph of sintered specimens (h_o/d_o=0.75, 1.00, 1.25)

Table 2 Condition of experiment for torsional upset forging

Specimen size [h_o/d_o]	Punch velocity [mm/sec]	Friction factor	Angular velocity of die [rad/sec]
0.75	1.0	m=0.4	0, 0.122, 0.264, 0.446, 0.572, 0.723, 0.836, 0.968
1.0			
1.25			

After the forging, the specimens go through solution heat treatment, where they are heated to 510±5°C for 30 minutes, quenched, and then aged at 170±5°C for 18 hours.

5. Results and Discussion

Figure 4 shows the results of experiments under the condition of 1.0 in h_o/d_o and 30% in the compression ratio. It can be seen that there is distinct bulging in the case of the conventional upset forging, while bulging is considerably reduced in the case of the torsional upset forging. However, it is difficult to form cylindrical shape exactly because of difficulties in the determination of the concentricity and direction of lubricants.

(a) initial billet   (b) conventional upset forging   (c) torsional upset forging

Figure 4: Photograph of experimental results (h_o/d_o=1.0, γ=30%, ω=0.264).

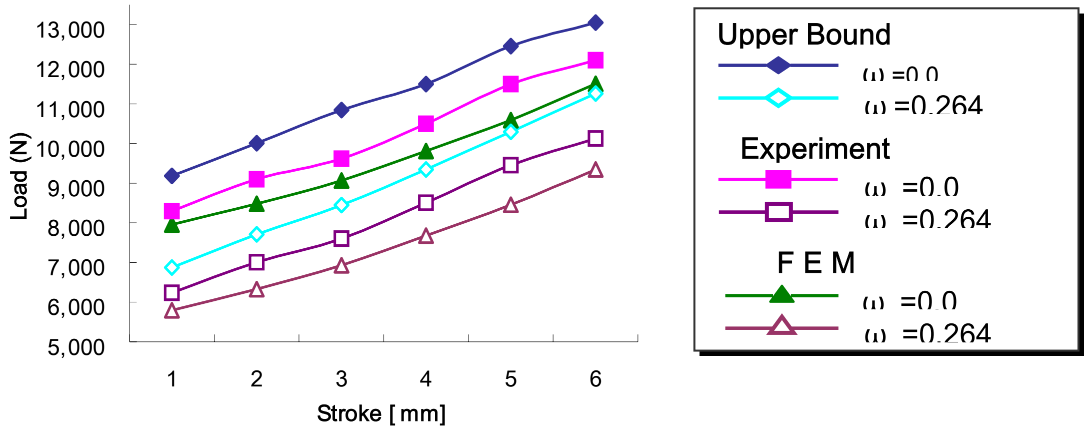

Figure 5: Result of forming load as a function of stroke (h_o/d_o=1.0, γ=30%, m=0.4)

Figure 5 shows the forming loads obtained by the upper bound analysis, the finite element simulation (DEFORM^{3D}), and experiments both for the conventional upset forging (ω=0.0) and the torsional upset forging (ω=0.264rad/s). The forming load during the conventional upset forging is 1.2ton, while that of the torsional upset forging is 1.0ton, which means 16% reduction in the forming load. Forming loads predicted by upper bound analysis are 1.305 and 1.126ton, which are in good agreement with experimental results.

Figure 6 shows the distribution of relative density by FE simulation. In the case of the conventional upset forging, the densification is the lowest near the die because of the friction effect. Near the bulging region, the densification is also low due to the nonvanishing circumferential tensile stress. Therefore, it is impossible to obtain overall uniform deformation because of a large difference in the relative density. In case of the torsional upset forging, however, there is more uniform distribution of relative density that is the most essential point in powder forging.

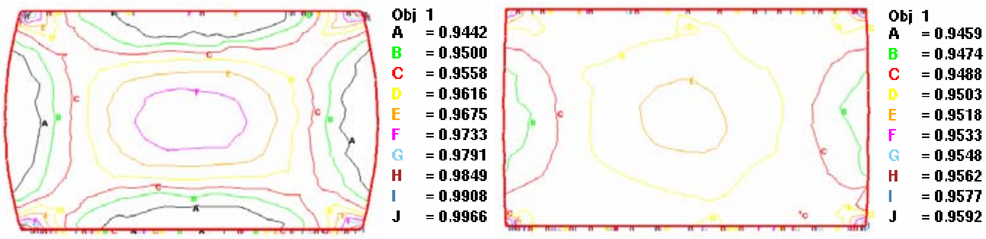

(a) conventional upset forging (b) torsional upset forging

Figure 6: Distribution of relative density (γ=30%, ω=0.446).

Figure 7 compares the distributions of effective strain during the conventional with the torsional upset forging. The effective strain at the central region in the case of the conventional upset forging is higher than in the torsional one and difference of effective strain over the whole area is lower in the torsional upset forging than in the conventional one, which indicates an improvement of the dead zone and an uniform deformation in the torsional upset forging. In other words, the rotation of the lower die makes dead metal zone between the die and the billet flow smoothly that results in reduction of the central zone.

Figure 8 shows the distribution of the maximum principal stress for the two cases. More uniform distribution is shown in the case of the torsional upset forging and it can reduce the difference of density in the sintered metal.

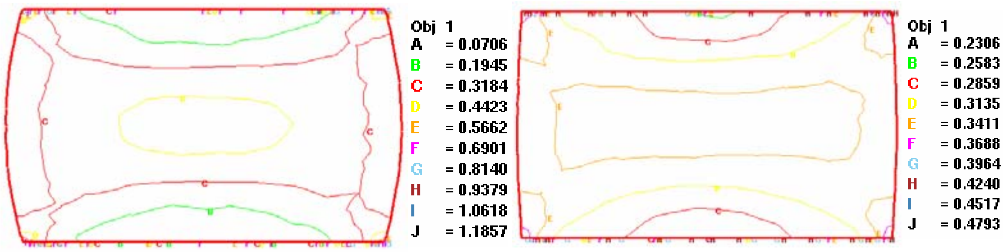

(a) conventional upset forging (b) torsional upset forging

Figure 7: Distribution of effective strain (γ=30%, ω=0.264).

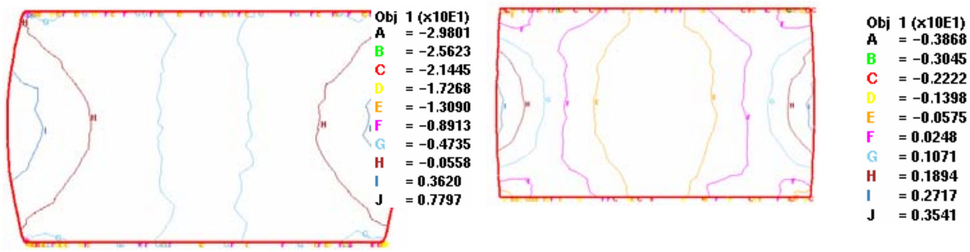

(a) conventional upset forging (b) torsional upset forging

Figure 8: Distribution of the maximum principal stress.

6. Conclusions

A torsional upset process of powder metal was studied and the following conclusions were obtained by comparing the results from the theoretical analysis and the FE simulation with those of experiments.

1. The torsional upset forging is able to reduce forming load compared with the conventional one.
2. By using the torsional upset forging, non-uniform deformation can be considerably reduced under the influence of rotation of the lower die.
3. The torsional upset forging leads to a twist shear deformation within the material, which is responsible for a relatively uniform distribution of the density or an improved densification.

References

[1] R. Duggirala and R. Shivpuri, “Effects of Processing Parameters in P/M Steel Forging on Part Properties: A Review – part Ⅱ Forging of Sintered Compact,” Journal of Materials Engineering and Performance, vol.1, 505-516, 1992.

[2] K. M. Xue, Y. Lu, H. H. Lin, and X. M. Zhao, “Numerical simulation and experimental research into the process of twist-compression forming”, Advanced Technology of Plasticity, 1065-1070, 1993.

[3] J.H. Park, Y.H. Kim, and Y.E. Jin, "Experimental Investigation of the Forming Parameters of the Rotational Upset Forging Process", Journal of Materials Processing Technology, vol.111, 103-106, 2001.

[4] X. Kemin W. Zhen and L. Yan, “FEM Analysis of Cylinder Twist-Compression deformation regularity”, Journal of Material Processing Technology vol.69, 103-106, 2001.

[5] Y.H. Kim, J.H. Park, and Y.E. Jin, "An Analysis of Plastic Deformation Processes for Twist-Assisted Upset Forging of Cylindrical Billets", Journal of Engineering Manufacture, Part B, Proceedings of the Institution of Mechanical Engineers, vol.215, no.6, 883-886, 2001.

[6] X.Ma, M.R. Barnett, and Y.H. Kim," Deformation Behaviour of a Cylinder under Simultaneous Compression and Torsion", Key Engineering Materials, vol.233-236, 767-772, 2002.

[7] S. Shima and M. Oyane, “Plasticity Theory for Porous Metals”, International Journal of Mechanical Science, vol.18, 285-291, 1976.